



## NRC Publications Archive Archives des publications du CNRC

### **Laser-ultrasonic measurements of residual stresses in a 7075-T651 aluminum sample surface-treated with low plasticity burnishing** Moreau, A.; Man, C.-S.

This publication could be one of several versions: author's original, accepted manuscript or the publisher's version. / La version de cette publication peut être l'une des suivantes : la version prépublication de l'auteur, la version acceptée du manuscrit ou la version de l'éditeur.

For the publisher's version, please access the DOI link below. / Pour consulter la version de l'éditeur, utilisez le lien DOI ci-dessous.

#### **Publisher's version / Version de l'éditeur:**

<https://doi.org/10.1063/1.2184692>

*Review of Progress in Quantitative Nondestructive Evaluation: volume 25:  
Brunswick, Maine, 31 July - 5 August 2005, 2006-03-06*

#### **NRC Publications Record / Notice d'Archives des publications de CNRC:**

<https://nrc-publications.canada.ca/eng/view/object/?id=6d610735-b0f2-4de6-b15e-2b1a51035e56>

<https://publications-cnrc.canada.ca/fra/voir/objet/?id=6d610735-b0f2-4de6-b15e-2b1a51035e56>

Access and use of this website and the material on it are subject to the Terms and Conditions set forth at

<https://nrc-publications.canada.ca/eng/copyright>

READ THESE TERMS AND CONDITIONS CAREFULLY BEFORE USING THIS WEBSITE.

L'accès à ce site Web et l'utilisation de son contenu sont assujettis aux conditions présentées dans le site

<https://publications-cnrc.canada.ca/fra/droits>

LISEZ CES CONDITIONS ATTENTIVEMENT AVANT D'UTILISER CE SITE WEB.

**Questions?** Contact the NRC Publications Archive team at

PublicationsArchive-ArchivesPublications@nrc-cnrc.gc.ca. If you wish to email the authors directly, please see the first page of the publication for their contact information.

**Vous avez des questions?** Nous pouvons vous aider. Pour communiquer directement avec un auteur, consultez la première page de la revue dans laquelle son article a été publié afin de trouver ses coordonnées. Si vous n'arrivez pas à les repérer, communiquez avec nous à PublicationsArchive-ArchivesPublications@nrc-cnrc.gc.ca.



imi 2005-111914-9  
CNRC 48837

## LASER-ULTRASONIC MEASUREMENTS OF RESIDUAL STRESSES IN A 7075-T651 ALUMINUM SAMPLE SURFACE-TREATED WITH LOW PLASTICITY BURNISHING

A. Moreau<sup>1</sup> and C.-S. Man<sup>2</sup>

<sup>1</sup>Industrial Material Institute, National Research Council of Canada,  
75 de Mortagne Boucherville, QC, Canada J4B 6Y4

<sup>2</sup>Department of Mathematics, University of Kentucky  
715 Patterson Office Tower, Lexington, KY 40506-0027

**Abstract.** Low-plasticity burnishing (LPB) is used to introduce deep compressive surface residual stresses that improve the durability of parts. A non-destructive measurement of residual stresses, their anisotropy, and distribution as a function of depth is being sought to verify initial process quality and residual stress retention over time. Laser-ultrasonic measurements of Rayleigh wave and surface skimming longitudinal wave (SSLW) velocities were used together to evaluate the magnitudes and directions of the two principal stresses independently of LPB-induced texture variations. The results agree with x-ray measurements at the surface. In addition, it was found that the laser-ultrasonic pulse generation mechanism was surface-process dependent.

**Keywords:** Residual stress, ultrasound, texture, LPB

**PACS:** 81.70.Cv, 62.20.-x, 62.20.Dc, 43.58.+z, 78.70.-g

### INTRODUCTION

Low-plasticity burnishing (LPB) is an emerging surface processing technique used to introduce deep compressive surface residual stresses that improve the durability of parts. With this technique, a ball or a roll applies pressure to the surface and compressive surface residual stresses are produced. These stresses vary in magnitude with depth and they may be anisotropic. A non-destructive measurement of the two principal components of residual stresses (amplitude and direction) and their variation as a function of depth is being sought to verify process quality and residual stress retention over time.

An early review of ultrasonic measurements of residual stresses may be found elsewhere [1]. In general, researchers have struggled with numerous difficulties. The first is that the crystallographic orientation distribution (texture) induces larger velocity variations than residual stresses. Consequently, texture-independent measurement configurations were found. Lately, the NDE community began considering that surface processing designed to induce residual stresses generally causes plastic flow of the material near the surface [2]. Plastic flow induces dislocations and stores energy. This promotes recovery and annealing and can cause a reduction of the residual stresses as the part ages at elevated temperatures

[2]. However, plastic flow also causes texture changes that affect the ultrasound velocity. This may explain why some previous work reported velocity variations of the opposite sign to what would be expected from residual stresses alone. Finally, texture also affects the acoustoelastic constants of the material [3]. However, this is a second order effect and it is almost always either neglected or taken into account empirically by measuring the acoustoelastic constants for each specific alloy and thermomechanical processing route. It is therefore essential to develop a measurement method that is insensitive to the texture variation induced by the surface process.

Other difficulties arising from ultrasonic measurements are the effects of surface roughness on the measured velocity [4,5] and diffraction effects [6]. Finally, if a depth profile of the residual stresses is to be obtained with a resolution of about one tenth of the maximum measurement depth, one can intuitively expect that the ultrasonic technique should have a measurement bandwidth that varies by at least one order of magnitude. To this end, laser-ultrasonics is one of the more promising candidate technologies because it is not-only wideband but also non-contact, versatile, and highly precise. Moreover, it is one of very few ultrasonic techniques that may eventually provide a lateral resolution of order one to a few mm in addition to depth resolution.

In this paper, ultrasonic measurements of Rayleigh surface waves and of surface skimming longitudinal waves (SSLW, also called P waves) are made over a wide bandwidth using laser ultrasonics. By using these two waves simultaneously, one can measure the change in residual stress and the change in texture produced by the LPB process. Surface roughness difficulties are avoided completely due to the mirror-like quality of the LPB surface. And diffraction effects are minimized by the measurement geometry. However, a new difficulty related to laser generation of ultrasound is encountered and solved. The measurements are used to predict surface residual stresses and these agree with x-ray measurements made at the surface. The interpretation of the data as a function of depth is outside of the scope of this paper.

## **EXPERIMENTAL PROCEDURE**

### **Test Sample**

A square sample of 10 cm to a side was cut from a 22.2 mm thick commercial plate of aluminum alloy 7075-T651. This designation indicates that after being rolled, the plate was *solution heat treated and artificially aged* to improve mechanical properties and dimensional stability [7]. The designation also indicates that, following the heat treatment, the plate was *stress-relieved by stretching*, i.e. stretched a small amount, of order 1.5 to 3%, to flatten the plate and relieve residual stresses. Furthermore, the two faces of the plate were ground away using a low-stress grinding process. The final sample thickness was 20 mm and the surfaces were quite smooth.

The LPB process was applied to one half of one of the two surfaces as shown in Fig. 1. The exact process parameters are proprietary, but for the purpose of this paper, it is sufficient to know that the process produced a mirror-like surface quality. Also, x-ray measurements indicate that the surface residual stresses were respectively  $-187 \pm 4$  MPa and  $-423 \pm 6$  MPa in the direction of the LPB process and perpendicularly.

### **Measurement system and setup**

Rayleigh and P wave velocities were measured using laser-ultrasonics. A general description of the technology and specific details regarding the measurement of Rayleigh and P waves can be found elsewhere [8,5]. The ultrasound source was a mode-locked laser focused to a line 2 to 5  $\mu\text{m}$  wide and approximately 5 mm long. The generation laser emitted ultraviolet (355 nm) pulses of 35 ps duration and energy less than 1 mJ/pulse. Detection involved an infrared (1.06  $\mu\text{m}$ ) long-pulse laser of 50  $\mu\text{s}$  pulse duration focused to a line approximately 2 mm long by 20  $\mu\text{m}$  thin and an InPFe photorefractive interferometer [9]. Shutters limited the repetition rate on the sample to 1 Hz to avoid heating the sample by the laser radiations and so obtain a velocity change caused by elastic constant variations with temperature.

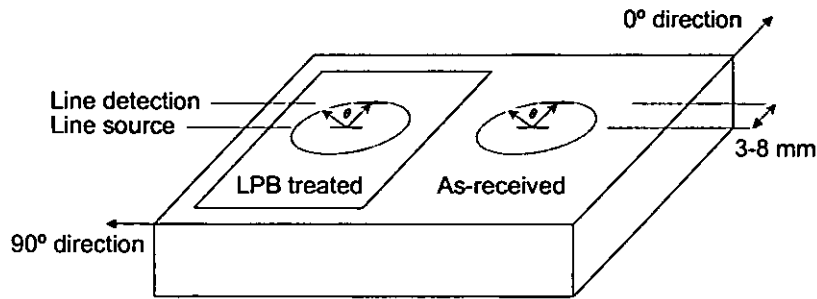


Figure 1. Schematics of the experimental measurement setup.

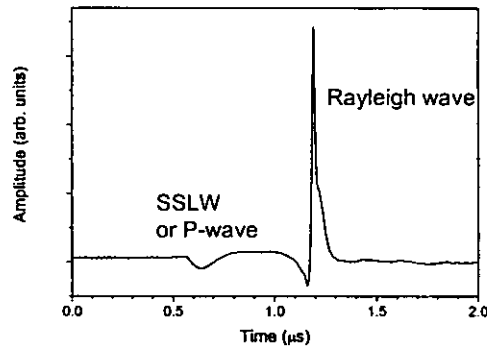


Figure 2. Surface displacement amplitude vs. time showing the SSLW and the Rayleigh wave pulses.

The standard separation distance between the two lines was 4 mm (Fig. 1). This distance was large enough to separate the Rayleigh and P waves and short enough to retain enough amplitude to measure the P wave with a good signal-to-noise ratio. Measurements were made as a function of angle ( $\theta$ ) with respect to the LPB processing direction, in steps of  $15^\circ$ , from  $0$  to  $195^\circ$ . In the  $180^\circ$  direction, measurements were also made in 1 mm increments, from 3 to 8 mm separation, to obtain the absolute sound velocity in that direction. The same procedure was applied on both an LPB-treated surface and on a non-treated surface of the same sample, approximately 5 cm away. It was assumed that the as-received surface texture and residual stresses did not vary significantly over such a short distance. A typical ultrasonic signal displaying the time of arrival of the P pulse (near  $0.6 \mu\text{s}$ ) and Rayleigh pulse (near  $1.2 \mu\text{s}$ ) is shown in Fig. 2. The P-wave and Rayleigh wave frequency contents are from 2 to about 15 MHz and 2 to more than 60 MHz, respectively.

## DATA REDUCTION

The objective is to calculate the relative change of ultrasound velocity caused by the LPB process as a function of propagation direction,  $\theta$ , and frequency,  $f$ , i.e. to calculate  $\Delta V(\theta, f)/V_0$  where  $V_0$  is the sound velocity in a hypothetical material with isotropic texture and no internal stresses. First, the isotropic velocity is estimated from the propagation delay as a function of distance from the measurements taken in the  $180^\circ$  direction. Because the material is likely not isotropic and stress free, the estimated  $V_0$  may have an error of a few percent. However, this will yield only a systematic and negligible error in  $\Delta V(\theta, f)/V_0$ . For two propagation distances,  $x_1$  and  $x_2$ , the Rayleigh or the P ultrasonic pulse is windowed and Fourier transformed, thus yielding an amplitude and phase for each frequency component. The phase difference between the two propagation distances is computed and converted to a propagation delay,  $\Delta t(f)$ . From this we estimate  $V_0(f) = (x_2 - x_1)/\Delta t(f)$ .

Two different methods were utilized to calculate  $\Delta V(\theta, f)/V_0$  in the  $\theta = 180^\circ$  direction: these will be called the 4-measurements and the 2-measurements methods. In the 4-measurements method,  $V(f)$  is calculated on each surface using measurements at two different propagation distances and the Fourier method described above. The quantity  $\Delta V(f)/V_0$  is calculated simply by subtracting the two velocity spectra and normalizing by  $V_0$ . This is repeated for each of the two surfaces and, therefore, requires four distinct

measurements. In the 2-measurements method, the propagation delay between the source and the receiver,  $\Delta t(f)$ , is measured for only one propagation distance on each of the two surfaces. The relative velocity variations are obtained by calculating

$$\frac{\Delta V}{V_0} = \frac{1}{V_0} \left( \frac{x}{t''} - \frac{x}{t'} \right) \approx -\frac{\Delta t}{t'} = -\frac{V_0 \Delta t}{x}, \quad (1)$$

where the prime and double prime refer to the as-received and LPB-treated surfaces, respectively,  $x$  is propagation distance, and  $\Delta t = t'' - t'$ . The two methods are illustrated schematically in Fig. 3. They should yield identical results but Fig. 4 shows that they do not. Worse, the result of the 2-measurement method depends on propagation distance. This discrepancy is also observed when calculating  $\Delta V(f)/V_0$  for the P waves (not shown)

Ultrasound was generated near the threshold between the thermoelastic and ablation regimes. If ablation did occur, the surface could be modified and the ultrasound source might vary. But the pulse shapes did not change after more than 100 consecutive measurements. However, close inspection revealed that the generated ultrasonic pulses were not exactly identical on the LPB-treated and as-received surfaces, as shown in Fig. 5.

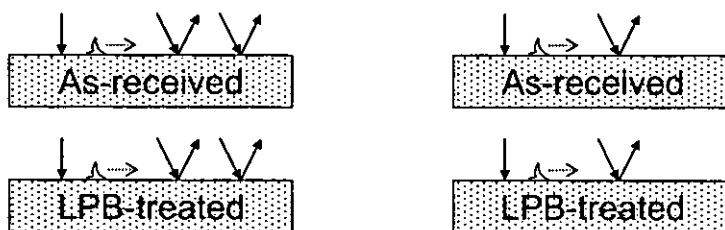


Figure 3. Schematics of the 4-measurement method (left) and 2-measurement method (right).

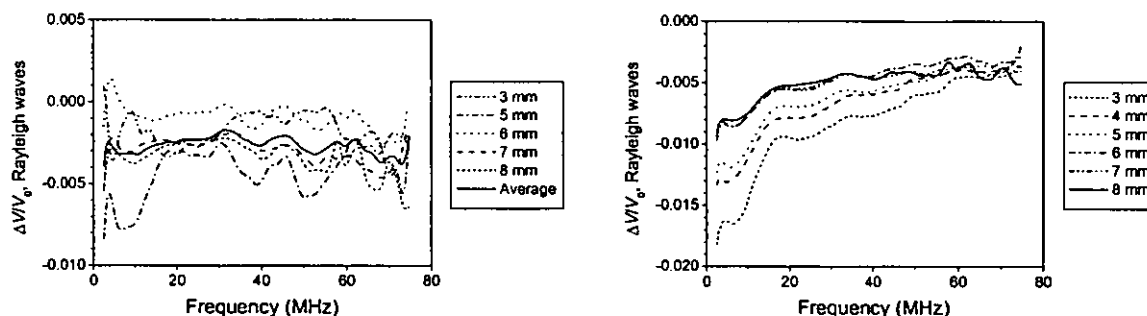


Figure 4.  $\Delta V(f)/V_0$  using the 4-measurements method (left) and the 2-measurements method (right). For the 4-measurement method, one of the two measurement distances was 4 mm and the other is indicated in the legend. For the 2-measurement method, the propagation distance is indicated in the legend.

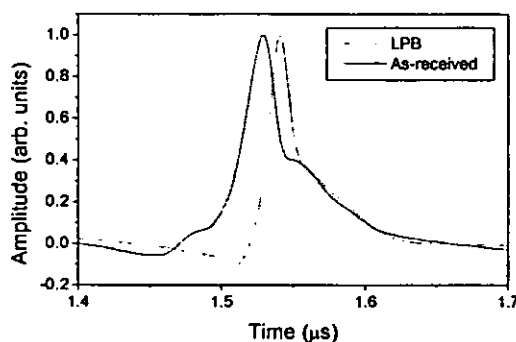


Figure 5. Comparison of the Rayleigh pulse waveforms generated on the as-received and LPB surfaces. The waveforms are scaled so that the maximum amplitude is 1.



Pulse shape depends on both the amplitude and the phase spectrum of the waveform. However, if the pulses from the two surfaces differ in the amplitude spectra, the estimated values of  $\Delta V(f)/V_0$  would not be affected. Therefore, we hypothesize that the acoustic pulses generated on the two surfaces do not have the same phase spectra. More specifically, we hypothesize that the laser-generated acoustic pulse has a frequency-dependent delay (or phase shift) characteristic of the laser-surface interaction. This generation delay spectrum can be measured by acquiring pulses having propagated 2 different propagation distances, and back-propagating these pulses to the source. Then, the difference between the generation delay spectra of the two surfaces can be calculated and this difference can be used to systematically correct all subsequent measurements using the 2-measurement method. The results obtained using this *corrected* 2-measurement method are shown in Fig. 6. There is no more dependence with propagation distance and the results agree with those obtained using the 4-measurement method.

It was also assumed that the correction did not depend on the orientation of the laser line source with respect to the sample. This allowed to calculate  $\Delta V(\theta, f)/V_0$  for all values of  $\theta$  using the corrected 2-measurement method (Fig. 7). The procedure was also repeated for the P waves. In this case, however, the correction was difficult to evaluate with the available data. Fig. 7 shows that the relative velocity change of the Rayleigh and P wave increase in the  $90^\circ$  direction (direction transverse to the LPB process). The frequency dependence of the P waves is not large enough as compared to the measurement precision to conclude that it is significantly different from zero. The frequency dependence of the Rayleigh waves is significant at low frequencies but possibly not above approximately 20 MHz. There are two possible reasons to expect this. First, diffraction effects are most important below 10 MHz and negligible at high frequencies. Second, at high enough frequencies, the waves are contained within the strained layer and do not penetrate into the bulk of the material. As an order of magnitude estimate, the wavelength and penetration depth of Rayleigh surface waves is approximately  $100 \mu\text{m}$  at 30 MHz. On the other hand, the penetration depth of P waves is an open problem and we will assume here that P waves have the acoustic properties of the surface.

Restricting our objective to the measurement of the residual stresses at the surface, the frequency dependence will be neglected.  $\Delta V/V_0$  is averaged in the 20-60 MHz frequency bandwidth for the Rayleigh waves and in the 3-12 MHz frequency bandwidth for the P waves. These are plotted and least-squares fitted to Eq. (4) in Fig. 8. The measurement errors are smaller for the Rayleigh waves because these waves are measured with a better signal-to-noise ratio. However, the velocity variations of the P wave are larger. Fig. 8 shows that Rayleigh and P waves velocities have extrema at different angles.

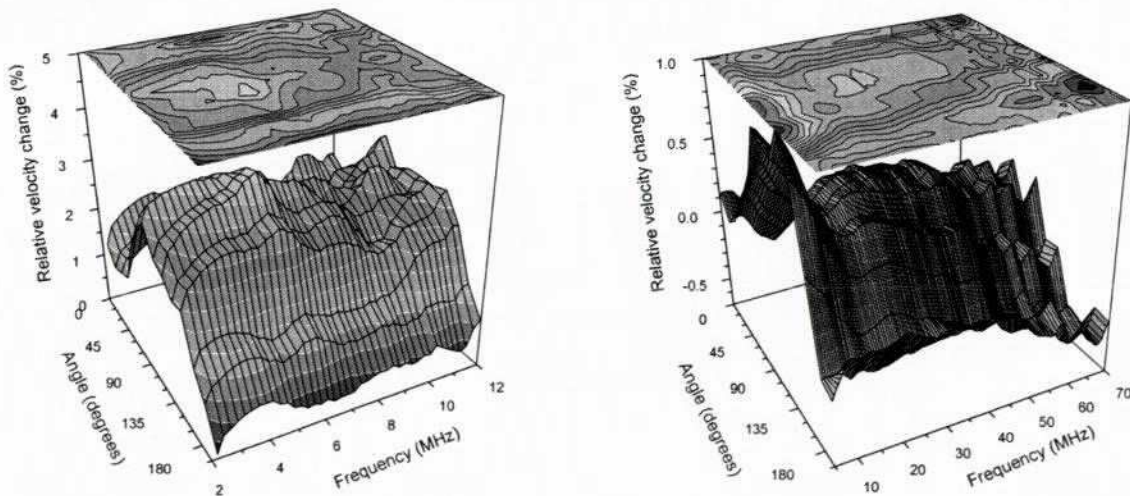


**Figure 6.** Corrected relative velocity change between the as-received and LPB-treated surfaces using the 2-measurements analysis. The average of all curves of Fig. 4 (left) is also shown in solid black for comparison.

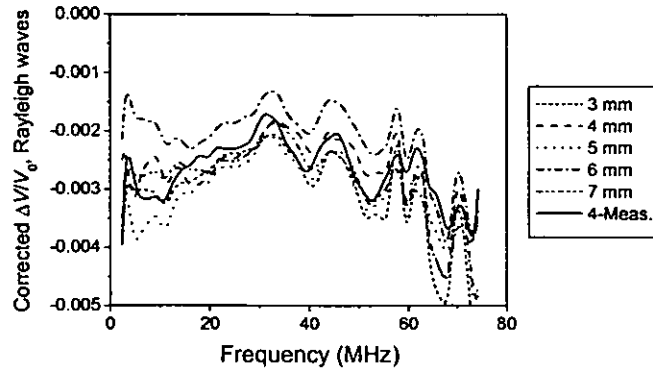


Figure 7. Relative velocity change of the P waves (left) and Rayleigh waves (right) between the as-received and LPB-treated surfaces as a function of frequency and angle.

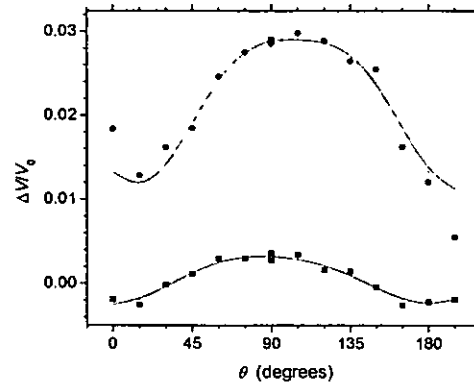


Figure 8. Square symbols: Measured angular variation of  $\Delta V_R/V_{R0}$  in the 20-60 MHz bandwidth. Circular symbols: Measured angular variation of  $\Delta V_P/V_{P0}$  in the 3-12 MHz bandwidth. The lines are the fitted model.

## ULTRASOUND MODEL AND INVERSE PROBLEM

The details of the mathematical model are found elsewhere [10]. In summary, we assume that the material is a polycrystalline aggregate of cubic material with overall orthorhombic symmetry. Let the normal direction to the free surface be the 3-axis, and the reference (rolling) direction in the plane of the surface be the 1-axis. Then, the model predictions of the Rayleigh wave velocity,  $V_R$ , and of the P wave velocity,  $V_P$ , are

$$\frac{V_R - V_{R0}}{V_{R0}} = \alpha_R W_{400} + \beta_R W_{420} \cos 2(\theta - \theta_w) + \gamma_R W_{440} \cos 4(\theta - \theta_w) + \delta_R T_m + \varepsilon_R T_d \cos 2(\theta - \theta_{RS}), \quad (2)$$

$$\frac{V_P - V_{P0}}{V_{P0}} = \alpha_P W_{400} + \beta_P W_{420} \cos 2(\theta - \theta_w) + \gamma_P W_{440} \cos 4(\theta - \theta_w) + \delta_P T_m + \varepsilon_P T_d \cos 2(\theta - \theta_{RS}), \quad (3)$$

where the subscripts  $R0$  and  $P0$  refer to the velocities in a material with isotropic texture and no residual stresses,  $\theta$  is the angle between the propagation direction and the 1-axis,  $\theta_w$  is the angle between the reference direction of texture and the 1-axis,  $\sigma_a$  and  $\sigma_b$  are the principal stresses in the (principal)  $a$ - and  $b$ -direction, respectively,  $\theta_{RS}$  is the angle between the  $a$ -direction and the 1-axis,  $T_m = (\sigma_b + \sigma_a)/2$ ,  $T_d = (\sigma_b - \sigma_a)/2$ . The  $W_{4m0}$  coefficients are the fourth-order crystallographic orientation distribution coefficients. The Greek letter symbols depend on single crystal elastic properties. They can either be obtained from micromechanical models or from calibration experiments. These equations are used to calculate the relative change of the Rayleigh wave velocities,  $\Delta V_R/V_{R0}$  and  $\Delta V_P/V_{P0}$ , respectively, caused by surface processing. After algebraic manipulations, one finds that

$$\Delta V_R/V_{R0} = (V''_R - V'_R)/V_{R0} = A_R + B_R \cos 2\theta + C_R \sin 2\theta + D_R \cos 4\theta + E_R \sin 4\theta \quad (4)$$

where the parameters  $A_R$  through  $E_R$  are combinations of the material parameters  $\alpha_R$  to  $\varepsilon_R$ , the  $W_{400}$ ,  $T_m$  and  $T_d$ ,  $\theta_W$  and  $\theta_{RS}$ , and where the prime and double prime refer to the material before and after LPB processing, respectively. Another equation is obtained for  $\Delta V_P/V_{P0}$  where the subscripts  $R$  are replaced by  $P$ . Eq. (4) can be fitted to the data using a simple multiple linear least squares fit. The expressions for the fitted parameters  $A$  to  $E$  are inverted to obtain the following information about changes in residual stresses and texture:

$$\Delta T_m = T''_m - T'_m = \frac{\alpha_P A_R - \alpha_R A_P}{\alpha_P \delta_R - \alpha_R \delta_P} \quad \text{and} \quad \Delta W_{400} = W''_{400} - W'_{400} = \frac{\delta_P A_R - \delta_R A_P}{\alpha_R \delta_P - \alpha_P \delta_R}; \quad (5)$$

and if it can be assumed that  $T'_d = 0$ , then

$$\theta''_{RS} = \frac{1}{2} \arctan \left( \frac{\beta_R C_P - \beta_P C_R}{\beta_R B_P - \beta_P B_R} \right), \quad (6)$$

$$T''_d = \frac{\beta_R B_P - \beta_P B_R}{(\beta_R \varepsilon_P - \beta_P \varepsilon_R) \cos 2\theta''_{RS}} = \frac{\beta_R C_P - \beta_P C_R}{(\beta_R \varepsilon_P - \beta_P \varepsilon_R) \sin 2\theta''_{RS}}. \quad (7)$$

These equations are completely decoupled from texture modification that could arise at the surface from the LPB process. Note that only the  $2\theta$  dependence of the ultrasound velocity is required to characterize the residual stress anisotropy. However, the  $B$  and  $C$  parameters cannot be evaluated simultaneously without evaluating  $A$  and at least one of  $D$ ,  $E$ , or some combination of  $D$  and  $E$ . Therefore, measurements at four different angles are necessary and sufficient to evaluate  $T''_m$ ,  $T''_d$ , and  $\theta''_{RS}$ . One such set of four measurements would be in the directions of  $\theta = 0, \pi/4, \pi/2$ , and  $3\pi/4$ .

## DISCUSSION

The fitted values (from Fig. 8) of parameters  $A$  through  $E$  were substituted into Eqs. (5-6) to estimate  $T''_m$ ,  $T''_d$ , and  $\theta''_{RS}$ . The ultrasonically measured mean residual stress induced by the LPB process is compressive and equal to  $T''_m = -498$  MPa. X-ray measurements of the surface residual stresses gave  $T''_m = -305$  MPa. Although the agreement may seem poor at first, this is an excellent result. Referring to Eq. (5), we see that  $T''_m$  is highly sensitive to errors in  $A_P$ , a value that was relatively inaccurate in our measurements because of the large uncertainties involved in correction applied to the 2-measurements method for the effect of surface processing on the generated acoustic P pulse (the correction for the Rayleigh pulse was much more accurate). However, it is quite possible that future development in laser ultrasonic technology will provide a much more accurate value of  $A_P$  because the source of inaccuracy is now well understood. The result is also excellent because measurement involving Rayleigh waves only have notoriously failed in the past. Most likely they have failed because they did not take into account texture changes near the surface. In contrast, our measurements account for the effects of texture.

The ultrasonic values of  $\theta''_{RS} = 12.4^\circ$  and  $T''_d = -143$  MPa indicate that the residual stresses are anisotropic, that the principal axis of  $\sigma_a$  is  $12^\circ$  from the LPB rolling direction, which is also the plate rolling direction. The measured x-ray value  $(\sigma_2 - \sigma_1)/2 = -118$  MPa is in general not equal to  $T''_d = (\sigma_b - \sigma_a)/2$  because  $\sigma_2$  and  $\sigma_1$  are in the LPB-rolling and transverse direction whereas the ultrasonic measurements indicate that  $\sigma_b$  and  $\sigma_a$  are  $12^\circ$  away from those directions. However, we calculate from the ultrasonic data that  $(\sigma_2 - \sigma_1)/2 = \frac{1}{2} (\sigma_b - \sigma_a) \cos 2\theta''_{RS} = -130$  MPa. This agrees with the x-ray value to within 10%.

\* Hole drilling measurements obtained post conference by P. Bouchard & A. Moreau of CNRC-IMI gave  $T''_m \sim -470$  MPa,  $|T''_d|$  decreases from 110 to 10 MPa, and  $\theta''_{RS} \sim 10^\circ$  in the first 500  $\mu\text{m}$  below the surface.



## CONCLUSION

It was shown that laser-generated ultrasound pulses had a phase spectrum that depends on the nature of the material's surface. Consequently, to obtain an accurate measurement of ultrasound velocity, it is necessary to either 1) make a measurement that is independent of the source, as in the 4-measurement method, or 2) characterize the source and apply the necessary correction to the data, as in the corrected 2-measurement method.

Measurements of magnitude and direction of the two principal axes of residual stresses were obtained independently of texture and of texture modifications that the LPB process may have caused. These measurements were obtained within the relatively general assumption that the overall texture anisotropy is orthorhombic with one axis of symmetry being perpendicular to the surface normal. It was also assumed that the as-received surface was free of residual stresses. No assumption was made regarding the orientation of the symmetry axes of texture and residual stresses in the plane of the plate.

The obtained measurements agreed with x-ray measurements of residual stresses on the treated surface. Detailed x-ray measurements of residual stresses and texture as a function of depth are planned. The available frequency information of the ultrasonic measurements has not yet been utilized to characterize the depth profile. Once both the x-ray and ultrasonic analyses are fully completed, a more accurate comparison of x-ray and ultrasonic capabilities will be possible.

## ACKNOWLEDGEMENT

The authors thank Dr. Michael J. Shepard of the U.S. Air Force Research Laboratory for valuable discussions and for the aluminum sample used in this work. The research reported here was supported in part by a DEPSCoR grant from AFOSR (No. F49620-02-1-0243), and in part by a grant from the Kentucky Science and Engineering Foundation as per Grant Agreement #KSEF-148-502-02-19. The research efforts of Man were also partially supported by a grant from the U.S. National Science Foundation (No. DMS-0406004).

## REFERENCES

1. Y.-H. Pao, W. Sachse, and H. Fukuoka, "Acoustoelasticity and Ultrasonic Measurements of Residual Stresses" in *Physical Acoustics* Vol. XVII, W. P. Mason and R. N. Thurston, eds. (Orlando, Academic Press, 1984) 61-143.
2. Metals Handbook Ninth Edition (Metals Park OH, American Society for Metals, 1982) Vol. 5, 138-149.
3. C.-S. Man, *Nondestr. Test. Eval.* **15**, 191-214 (1999).
4. A. G. Eguluz and A. A. Maradudin, *Phys. Rev. B* **28** (2) 728-747 (1983).
5. C. Bescond et al., "Determination of residual stresses using laser-generated surface skimming longitudinal waves" in *Proc. SPIE Vol. 5767, Nondestr. Eval. and Health Monitoring of Aerospace Mat., Composites, and Civil Infrastructure IV*. P. J. Shull, A. L. Gyekenyesi and A. A. Mufti, eds. (SPIE The Internat. Soc. for Opt. Eng., 2005) 175-186.
6. T. L. Szabo, "Anisotropic Surface Acoustic Wave Diffraction" in *Physical Acoustics* Vol. XIII, W. P. Mason and R. N. Thurston, eds. (New York, Academic Press, 1977) 79-113.
7. H. E. Boyer and T. L. Gall, eds., *Metals Handbook Desk Edition* (Metals Park OH, American Society for Metals, 1985).
8. B. Chenni, A. Moreau and J. Pouliquen, "NDE of Zinc Layer on Steel Substrate Using Laser-Ultrasonic SAW" in *Proc. SPIE Conf. on NDE for Health Monitoring and Diagnostics – Nondestr. Eval. & Reliability of Micro and Nanomaterial Systems*. (SPIE The Internat. Soc. for Opt. Eng., 2002) 14-20.
9. P. Delaye et al., *J. Optical Soc. Am. B* **14**, 1-12 (1997).
10. A. Moreau and C.-S. Man. *Proc. of MS&T Conf. 2005*. In print.